Langmuir

Article

pubs.acs.org/Langmuir

Resolving Self-Assembly of Bile Acids at the Molecular Length Scale

Larissa Schefer, Antoni Sánchez-Ferrer, Jozef Adamcik, and Raffaele Mezzenga*

Food and Soft Materials Science, Institute of Food, Nutrition and Health, ETH Zurich, Schmelzbergstrasse 9, LFO E23, CH-8092 Zürich, Switzerland

Supporting Information

ABSTRACT: The self-assembly behavior of the naturally occurring steroidal bile compounds cholic, deoxycholic, ursodeoxycholic, and lithocholic acid was studied by combining atomic force microscopy (AFM), polarized optical microscopy (POM), Fourier-transform infrared spectroscopy (FTIR), absorption spectroscopy (UV−vis), circular dichroism (CD), and wide-angle X-ray scattering (WAXS). Molecular solutions of these mono-, di-, and trihydroxyl substituted bile acids spontaneously evolved into supramolecular aggregates upon the incremental addition of H_2O as a poor solvent. Highly crystalline nanostructured multilayered assemblies were formed, which revealed a very rich polymorphism of micro- and macro-structures depending on the chemical structure of the bile acid and the properties of the cosolvent (EtOH or DMSO) used. In particular, AFM allowed resolving the crystalline structure to an unprecedented level. It was thus possible to establish that bile acids associate into H-bonded chiral dimer building blocks, which organize in 2D layers of nanostructured lamellar surface topologies with unique facial amphiphilicity. The detailed understanding of the hierarchical organization in bile acid assemblies may contribute to develop strategies to design bioinspired materials with tailor-made nanostructured surface topologies.

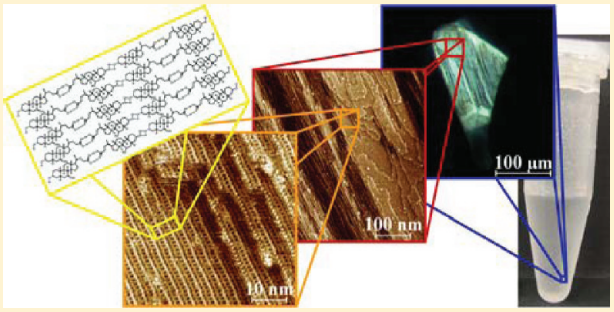

INTRODUCTION

Bile acids (BAs) are naturally occurring steroidal biodetergents, having diverse physiological functions in biologically relevant processes.[1,2] BAs consist of a chiral saturated tetracyclic steroidal skeleton containing one or more hydroxyl groups (OH), connected to a short chiral aliphatic chain with a carboxylic end group.[3] The *cis* configuration of the rings, which imposes a slight curvature of the rigid steroidal backbone, combined with the polar OH groups pointing toward the center of the concave α-face, and with the apolar methyl groups on the convex β-face, creates a unique facial amphiphilicity.[3]

The self-assembly of BAs in aqueous solutions is driven by both hydrophobic association of the apolar β-faces and H-bonding interactions from the OH groups on the polar α-faces and acid groups.[4] The number and conformation of OH groups greatly influence the solubility and association behavior of BAs.[5] Systems containing steroidal bile compounds have been reported to establish a wide number of different association modes by varying concentration, ionic strength, pH, and temperature.[4] The mechanisms responsible for this very rich polymorphism presumably arise from combined electrostatic, hydrophilic/hydrophobic, and H-bonding interactions. Molecular solutions were reported to transform into micelles,[6] nanotubes,[7,8] and twisted[7] or helical[9−11] fibrillar supramolecular structures. Depending on the solvent quality, steroidal molecules were found to spontaneously self-assemble into colloidal spheres, platelets, or helical ribbons.[12] Certain steroidal compounds are known for their solvent-specific gelation ability in both organic[13] and aqueous[14] media. X-ray diffraction experiments on fibrillar structures drawn from such gels revealed an elongated helical configuration of hexagonally packed nanofibers.[15,16] The potential of BAs as host molecules for the inclusion of a wide variety of organic molecules was also assessed by single-crystal X-ray crystallographic studies.[17−19]

Owing to characteristics such as amphiphilicity, chirality, high structural rigidity, biocompatibility, and ability to recognize organic molecules according to size, shape, polarity, and chirality, BAs and their derivatives are ideal building blocks for the construction of supramolecular assemblies. Many recent studies have shown their great potential for host−guest chemistry, biomimetics, molecular recognition, artificial receptors and transmembrane carriers for anions, drug delivery, and future biomaterials.[20−22] Yet, the potential proposed spectrum of supramolecular BA assemblies needs further elucidation of its self-association principles on a very fundamental level ranging from nano- to macro-scale.

The structural arrangement of self-assembled BA molecules can be tuned by varying the number, position, and stereochemistry of the OH groups in the BAs, as well as the solvent quality in which their aggregation occurs. Considering all these factors, naturally occurring lithocholic acid (LA), deoxycholic acid (DA), ursodeoxycholic acid (UA), and cholic acid (CA) were chosen as target molecules for the systematic study of the self-assembly of BAs (Scheme 1). Starting from molecular

Received: January 26, 2012
Revised: March 7, 2012
Published: March 13, 2012

   dx.doi.org/10.1021/la300384u | *Langmuir* 2012, 28, 5999−6005

Scheme 1. Chemical Structure of (a) Cholic Acid, (b) Deoxycholic Acid, (c) Lithocholic Acid, and (d) Ursodeoxycholic Acid

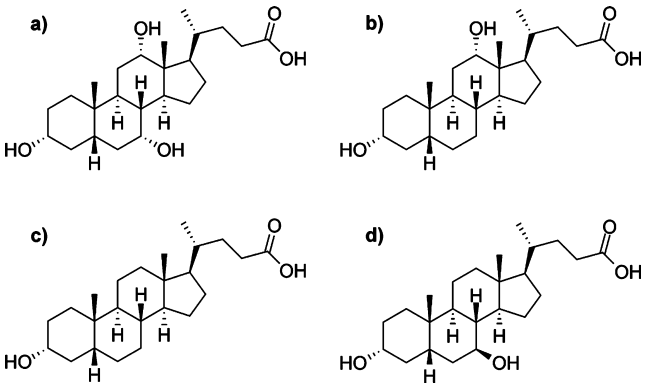

solutions in good solvents EtOH or DMSO, the aggregation of the respective BAs was induced by the incremental addition of H_2O as poor solvent. The hierarchical organization of the resulting aggregates from good/poor solvent mixtures was examined by combining polarized optical microscopy (POM), absorption spectroscopy (UV−vis), circular dichroism (CD), Fourier-transform infrared spectroscopy (FTIR), wide-angle X-ray scattering (WAXS), and atomic force microscopy (AFM) experiments. From these combined results, we were able to resolve the BAs self-association at the molecular length scale, demonstrating highly crystalline, hierarchical multilayered lamellar assemblies, with supramolecular head-to-head BA molecular packing, and we discuss next their complex architectures based on their spontaneous self-assembly behavior in solution.

EXPERIMENTAL SECTION

Materials. Cholic acid (CA) (3α,7α,12α-trihydroxy-5β-cholanic acid), deoxycholic acid (DA) (3α,12α-dihydroxy-5β-cholanic acid), lithocholic acid (LA) (3α-hydroxy-5β-cholanic acid), and ursodeoxycholic acid (UA) (3α,7β-dihydroxy-5β-cholan-24-oic acid) were obtained from Sigma-Aldrich and used as received. Ethanol (EtOH) and dimethyl sulfoxide (DMSO) were purchased from Merck and filtered by using 0.2 μm pore PTFE membranes. Ultrapure water (H_2O) was purified (18.2 MΩ·cm at 25 °C) from a Milli-Q integral water purification system (Millipore Corporation) and filtered through a 0.2 μm pore nylon membrane.

Sample Preparation. Molecular solutions of 1 wt % of each BA were prepared by dissolving the respective BA in EtOH or DMSO. The self-assembly behavior of the steroidal molecules was studied upon the dropwise addition of H_2O to the molecular BA solutions. The final mixtures consisting of 0.1 wt % BA in the good/poor solvent ratio (1:9) were vigorously vortexed and stored at room temperature. Liquid-state samples were studied as prepared and solid-state samples were obtained by recrystallization.

UV−Vis Spectroscopy and Circular Dichroism (CD). Molecular solutions of 0.1 wt % BAs in EtOH or EtOH/H_2O (1:9) were loaded into 1 mm Hellma 110-QS quartz precision cells and measured on a Jasco J-815 CD Spectrometer. UV−vis absorbance, high tension, and molar ellipticity signals were recorded from 700 to 190 nm with 1 nm intervals, and at the scanning speed of 100 nm·min^{-1} and 64 ms digital integration time in 3 accumulations at room temperature.

pH Meter. The pH values of all solutions were measured by a compact VWR International 1000 L precision pH meter at room temperature.

Fourier-Transform Infrared (FTIR) Spectroscopy. FTIR spectra in absorption mode were obtained by using a Varian 640 FTIR Spectrometer equipped with a Specac Diamond ATR Golden Gate. Solid-state samples were scanned over the range of 4000 to 600 cm^{-1} with a resolution of 2 cm^{-1} at room temperature and averaged over 256 scans.

Polarized Optical Microscopy (POM). The transparency/turbidity of samples was first inspected by eye under normal light conditions. The presence of birefringence was examined under crossed polarizers in transmission mode on a Zeiss Axioskop 2 MOT light microscope equipped with a color chilled Hamamatsu Photonics 5810 3CCD videocamera.

Atomic Force Microscopy (AFM). Sample solutions (30 μL aliquots) were deposited onto freshly cleaved Ted Pella 9.9 mm diameter mica disks, left to adsorb for 1 min at room temperature and dried smoothly with pressurized air. The surface topology of self-assembled BAs was analyzed on a Bruker Nanoscope VIII Multimode Scanning Force Microscope covered with an acoustic hood to minimize vibrational noise. The AFM was operated in tapping mode under ambient conditions using commercial silicon nitride cantilevers. Images were taken continuously at a scan rate of 0.3−0.5 Hz, and a number of pixels per image varying from 1024 × 1024 (low resolution) to 5120 × 5120 (high resolution). The images were flattened using the Bruker NanoScope 8.10 software, and no further image processing was carried out. Fast Fourier-transform (FFT) was performed using Wane Rasband ImageJ 1.45f software.

Wide Angle X-ray Scattering (WAXS). WAXS measurements were performed using a Rigaku MicroMax-002+ microfocused beam (4 kW, 45 kV, 0.88 mA). The Cu Kα radiation ($\lambda_{CuK\alpha}$ = 1.5418 Å) was collimated by three pinhole (0.4, 0.3, and 0.8 mm) collimators. Solid-state samples were probed over an effective scattering vector range of 0.15 nm^{-1} < q < 26.01 nm^{-1}, where q is the scattering wave vector defined as $q = 4\pi \sin\theta/\lambda_{CuK\alpha}$, with a scattering angle of 2θ. The scattered X-ray intensity signals were acquired by a Fuji Film BAS-MS 2025 imaging plate system (15.2 × 15.2 cm^2, 50 μm resolution).

RESULTS AND DISCUSSION

Micro- and Macroscopic Morphological Polymorphism of Self-Assembled Bile Acid Aggregates. Protonated BAs are known for their low solubility in water.[6] While trihydroxyl BAs can be made soluble by shifting the pH to basic conditions, di- and monohydroxyl BAs require strong alkali conditions or even the presence of solvents such as alcohols.[16] Therefore, molecular BA solution precursors were prepared by dissolving the corresponding BA in EtOH or DMSO. The self-assembly was induced by the dropwise addition of H_2O as poor solvent, giving the final good/poor solvent ratio of 1:9 and a final BA concentration of 0.1 wt %. The observation of turbidity due to the presence of suspended structures upon the addition of H_2O confirmed the aggregation of the BA molecules. LA solution samples turned turbid within a few minutes, solutions of DA and UA became turbid after hours, and solutions of CA after some days. Thus, decreasing the number of OH groups promotes aggregation. The number of OH groups affects the solubility in H_2O by acting as H-bonding sites and by shifting the hydrophilic/hydrophobic balance in the molecule.[5] Similar

dx.doi.org/10.1021/la300384u | Langmuir 2012, 28, 5999−6005

behavior was observed independently of the good solvent quality, that is in both EtOH and DMSO.

BA aggregates with different morphology appeared upon time depending on the chemical constitution of the BAs and the solvent quality (Figure 1). UV−vis experiments were first

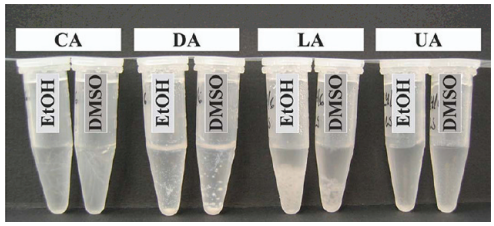

Figure 1. Macroscopic aggregate morphologies of 0.1 wt % BAs in good solvent/H_2O (1:9) assembled through the dropwise addition of H_2O to molecular solutions of cholic acid (CA), deoxycholic acid (DA), lithocholic acid (LA), and ursodeoxycholic acid (UA) in either EtOH (left sample) or DMSO (right sample).

performed in order to gain further insight into such aggregates (Supporting Information, Figure SI-1). CA formed flexible fibrillar aggregates already visible to the naked eye. The UV−vis spectra of this solution revealed no absorbance signal due to their precipitation from the solution medium. The opaque flake-like aggregates observed from DA, LA, and UA solutions exhibited increased absorption intensities upon decreasing wavelength as a result of the scattered light. Combined UV−vis and CD experiments allowed assessing the optical activity after aggregation. Molecular BA solutions showed a negative molar ellipticity signal at wavelengths below 250 nm along with the corresponding absorbance signal in the UV region which can be attributed to the absorption of the COOH group (λ_{max} = 230 nm).[23] A decrease of the molar ellipticity signal upon the addition of H_2O was observed confirming again the presence of aggregates which do not contribute to the molecular optical signal as a result of precipitation (Supporting Information, Figure SI-1).

Measuring the final pH media of aggregated samples allowed a better understanding of the underlying driving forces of the spontaneous self-assembly of BA molecules. Independently of the solvent mixture, the pH values remained rather constant for samples of the same BA. In contrast, the number of OH groups had a great effect on the final pH. The pH values gradually decreased with an increasing number of OH groups with the following sequence: LA (pH 6.7) > UA (pH 5.5) > DA (pH 5.1) > CA (pH 4.2). The acidity constants in water were reported to be the same for all BAs, independently of the number of OH groups in the molecular structure.[5] Assuming constant acidity strengths for all BAs - $pK_a \approx 5$ -,[24] an enhanced aqueous solubility due to a higher hydroxylation is expected to be the main responsible for the increased release of protons by BAs. Thus, the pH is lowered when BA molecules become more soluble in the order − CA > DA, UA > LA. In contrast, aggregates are consisting of protonated molecules, which do not contribute to the release of protons, and therefore these structures do not change the pH media. In other words, bile acids with an increased number of OH groups show a lower tendency to aggregate due to their enhanced solubility, and are more efficient to lower the pH by the release of protons from the carboxylic acid groups to the solvent media. The observation of the microstructure of the aggregates enables to elucidate the hierarchical configuration and complex architectures of their supramolecular structures. POM images of the aggregates provide a first insight into the structural arrangement on the microscale, which was found to vary among the BAs and cosolvents used (Figure 2). The presence of birefringence in all samples implies structural anisotropy (e.g., crystallinity) for all BA aggregates.

Bile Acids Associate into Building Blocks of H-bonded Dimers. A deeper understanding of the molecular association mechanisms of BA molecules can be provided by FTIR spectroscopy of their crystalline solid-state aggregates (Figure 3

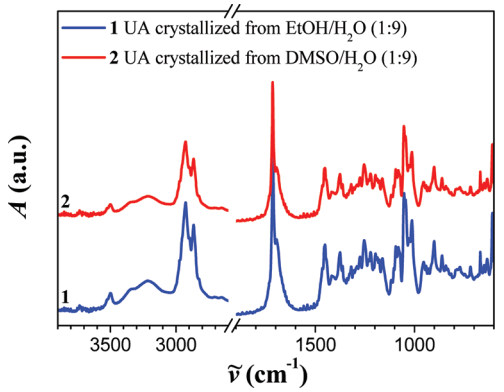

Figure 3. FTIR spectra of the solid-state ursodeoxycholic acid (UA) aggregates recrystallized by slow evaporation from EtOH/H_2O (1:9) and from DMSO/H_2O (1:9) solvent mixtures.

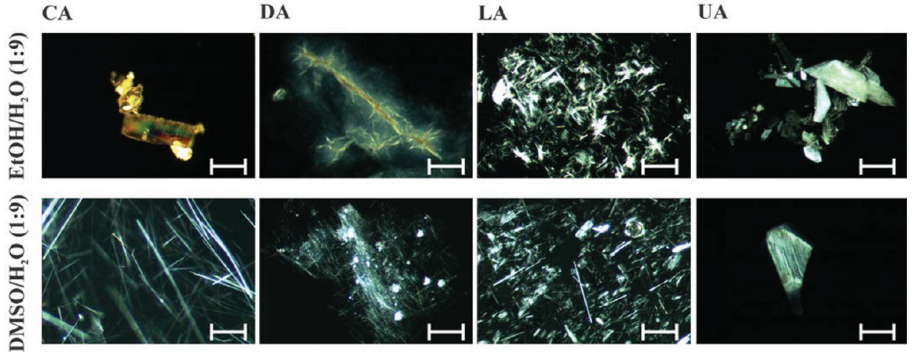

Figure 2. POM images of the cholic acid (CA), deoxycholic acid (DA), lithocholic acid (LA), and ursodeoxycholic acid (UA) aggregates from EtOH/H_2O (1:9) and DMSO/H_2O (1:9) under crossed polarizers showing birefringence. Scale bars correspond to 100 μm.

dx.doi.org/10.1021/la300384u | Langmuir 2012, 28, 5999−6005

and Supporting Information, Figure SI-2). The FTIR spectra of BAs can be divided into three main regions: (i) vibrational bands above 3100 cm^{-1} arising from O−H stretching, followed by (ii) the aliphatic C−H stretching appearing from 3000 to 2850 cm^{-1}, and (iii) sharp absorption peaks at 1712 (CA), 1694 (DA), 1699 (LA), and 1715 cm^{-1} (UA) assigned to the C═O stretching from COOH groups. Variations in the range above 3100 cm^{-1} are supposed to come from multiple contributing factors (i.e., the number of OH groups in the molecule, possible residual water content after recrystallization, H-bonding, and the formation of dimeric clusters) which might shift and broaden the absorption bands in this region.[25] The presence of sharp peaks above 3500 cm^{-1} is characteristic for unassociated OH groups, while broad peaks below this wavenumber range arise from associated forms of OH moieties.[25] It can thus be concluded that the majority of aggregated BA molecules established intermolecular H-bonding between the OH groups on the concave α-faces. However, some OH groups remained unassociated depending on the chemical structure of the BA compound. Assemblies which contain some free OH groups are present in the crystalline aggregates from the trihydroxyl BA (CA), as can be detected from the sharp peak in its FTIR spectra. Small sharp peaks are also present for the dihydroxyl BAs (DA and UA); the difference among these two compounds might be explained by the stereochemistry of OH groups which is out of plane in the case of UA. The absence of this sharp absorption peak in the case of monohydroxyl BA (LA) indicates the participation of its only OH group in H-bond formation. The carbonyl stretching from COOH groups at wavenumbers from 1715 to 1694 cm^{-1} corresponds to the H-bonded dimeric state of carboxylic acids in contrast to the carbonyl stretching of the monomeric COOH form appearing at around 1750 cm^{-1}.[25] Furthermore, the absence of the carbonyl stretching of carboxylates from 1610 to 1550 cm^{-1} also strongly indicates the presence of protonated BAs in the aggregates. These results are in agreement with the pH values and aggregation of BAs, mediated by intermolecular H-bonding of protonated carboxylic groups in a dimeric state.

Resolving Self-Assembly of the Crystals at the Molecular Length Scale. WAXS experiments were performed in order to identify the molecular packing of the structural anisotropic aggregates, which self-assembled from building blocks of dimeric BA molecules. Solid-state aggregates show characteristic WAXS scattering patterns with a multitude of sharp peaks indicating highly crystalline structures, as shown in Figure 4 and Supporting Information, Figure SI-3. Aggregates from UA yielded nearly invariant patterns, indicating a similar molecular arrangement independent of the cosolvent used. However, the patterns and thus the molecular packing do vary with the solvent quality for the other types of bile acids. Thus, different good solvents, EtOH and DMSO, promote different kinds of BA self-assembly. The architectures of the aggregates are highly complex as reflected by the multitude of reflections from WAXS spectra. The lowest detected q reflection of solid-state aggregated samples (labeled as q_1) varies from 4.2 to 7.0 nm^{-1} (d = 0.9−1.5 nm) and is in the same order of magnitude as the peaks from the corresponding commercial BA powders (Supporting Information, Table SI-1). In real space, this reflection indicates periodic features ranging from 0.9 to 1.5 nm, which compares well with the dimensions of BAs, whose long axis molecular length is about 1.4 nm (Supporting Information, Figure SI-4). Dimeric H-bonded molecules can indeed potentially associate in a layered manner, as suggested from FTIR experiments, but possible degrees of freedom arising from tilting, twisting rotation, and chirality of the BA dimers in the crystals make the resolution of the molecular packing structure within the repeat cell based solely on WAXS results challenging.

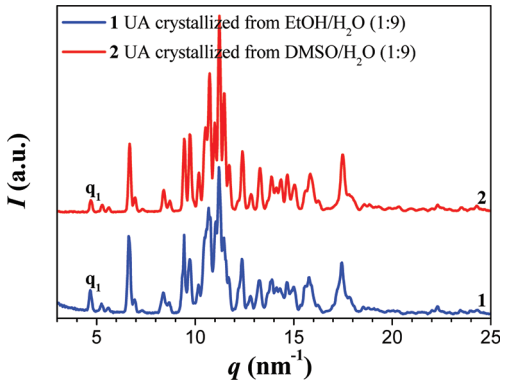

Figure 4. WAXS crystalline scattering patterns of the solid-state ursodeoxycholic acid (UA) aggregates recrystallized from EtOH/H_2O (1:9) and from DMSO/H_2O (1:9) solvent mixtures.

Additional insight into the complex architecture of supramolecular BA aggregates was gained by AFM. The surface topology of crystalline BA assemblies is illustrated by representative AFM phase images (Figure 5 and Supporting Information, Figures SI-5 to SI-11). Self-assembled structures from DA, LA, and UA are essentially arranged in manifold multilayers (the faces of CA aggregates, the most water-soluble BA considered, could not be sufficiently well resolved by the AFM). Nanostructured lamellae are observed on the surfaces of DA and UA recrystallized from DMSO; similarly LA recrystallized from both solvents exhibit highly crystalline faces, whereas the surface layers of DA and UA aggregates recrystallized from EtOH are rather flattened. These distinct regular lattices are furthermore observed to arrange in differently oriented lamellar domains (Supporting Information, Figures SI-6 and SI-8). Therefore, BAs hierarchically self-assemble into polydomains of lamellar lattices, resulting in multilayered crystalline aggregates. The observation of multilayers is in agreement with the multitude of sharp q reflections in WAXS patterns, indicating the presence of highly crystalline structures.

The layered surface of UA aggregates recrystallized from DMSO/H_2O reveals a hierarchically organized lattice of alternating lighter and darker lines, which appear to be somewhat interconnected and broken down by regular black cavities, as shown in Figure 5. The spacing between lighter and darker lines, as measured by FFT, is 1.5 nm which corresponds to half the distance between light lines measured to be 3.0 nm (Supporting Information, Figure SI-5). The lamellar nanostructures can only be observed on the declining aggregate face on the right part of the main AFM image. In contrast, the ascending face on the left AFM image side does not present a distinct lattice arrangement. The orientation of 3D randomly deposited BA aggregates is therefore crucial for the direct imaging of nanostructures, which may explain why the same highly hierarchical self-assembly is not resolved in DA and LA multilayer aggregates.

In a similar way, the small variations of the lattice spacing and other features size within the repeat unit observed for different BAs and solvents might be explained by the preparation of the sample, the exact plane observed, and the angle of observation

dx.doi.org/10.1021/la300384u | Langmuir 2012, 28, 5999−6005

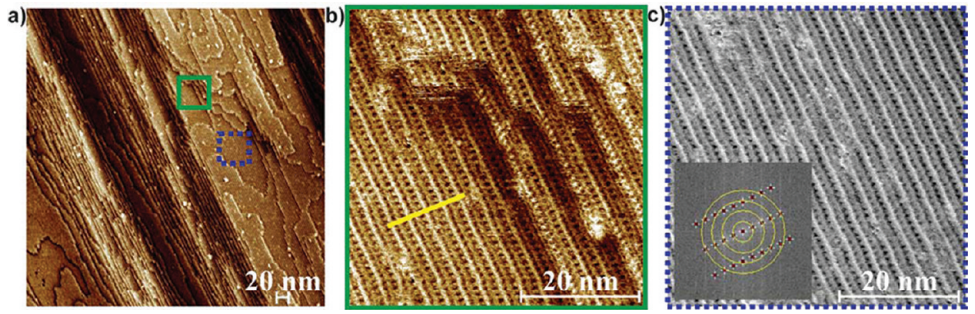

Figure 5. AFM phase images of self-assembled ursodeoxycholic acid (UA) from DMSO/H_2O (1:9). (a) Crystalline aggregates in arranged multilayers. (b) Zoom-in from the green square in panel a, showing nanostructured lamellae with a lattice spacing of 3 and 1.5 nm, respectively. (c) Zoom-in from the blue dotted square in panel a, with the corresponding FFT analysis as inset.

of the deposited 3D aggregates: any change in the above may induce a change in the resolution of the corresponding AFM mapping.

For the cases in which the smallest lattice spacing (1.0 to 1.7 nm) can be observed by both the FFT analysis on high resolution AFM images (d_{AFM}) and by WAXS measurements ($2\pi/q_1$), a good agreement between the two techniques is systematically found (Supporting Information, Table SI-2). The values of q_1 and its resulting real space distances $d = 2\pi/q_1$ can thus be identified with the spacing of lamellar structures observed by AFM, d_{AFM}, which in turn correspond closely to the molecular length of straight, or slightly tilted BA molecules (Supporting Information, Figure SI-4). This lattice spacing indicates a 1D longitudinally association of BAs, consistent with the lamellar layering observed. More specifically, the lattice spacing of 1.5 or 3.0 nm, observed for supramolecular UA aggregates from DMSO/H_2O (1:9), fits with the molecular length of a single BA molecule or to its intermolecular H-bonded dimeric state. Also supported by the FTIR results, the dimeric BA molecules are expected to self-assemble lengthwise in repeating units of H-bonded dimers, with intermolecular H-bonds between OH groups on the concave α-faces of the BA molecules. It is therefore the unique combination of hydrogen bonding and chirality which assists the hierarchical formation of the highly crystalline nanostructured 2D lamellar layers. The absence of WAXS reflections corresponding to the width of the dimeric BA molecules can arise by the nearly identical scattering length densities of the head and tail, dominated by OH and COOH, hydrogen bonded moieties. AFM experiments, on the other hand, can resolve specific interaction forces from differences in the surface topology. Depending on the 3D (chiral) orientation of dimeric molecules and the kind of intermolecular H-bonding, a lattice spacing of the molecular length or the dimeric unit can be mapped. The proposed lengthwise association via intermolecular H-bonding between terminal OH groups of H-bonded dimeric BA molecules is presented in Figure 6. Periodic lighter and darker lamellae are proposed to result from alternating oriented BA molecules presenting their concave α- and convex β-face, respectively. These molecules result arranged with a tilt angle of $\phi = 20°$ with respect to the normal to the lamellar layers, as evaluated by considering the spacing between layers (WAXS) and the long axis molecular length obtained by 3D chemical structures evaluation (Figure SI-4).

The supramolecular BA aggregates reported here self-assemble as a result of the different polarity, formation of H-bonds, and the hydrophilic/hydrophobic balance in the molecule, which allows their self-assembly into periodically

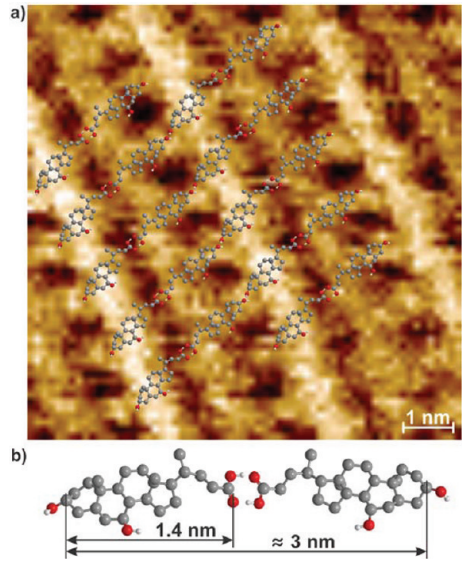

Figure 6. (a) Molecular arrangement of H-bonded dimeric bile acid (BA) molecules in self-assembled ursodeoxycholic acid (UA) recrystallized from DMSO/H_2O (1:9). The interlattice spacing of 3 nm fits with the molecular length of dimers, consisting of alternating concave- and convex-oriented BA molecules. (b) Detail of the self-assembling UA dimer unit with the corresponding feature dimensions.

nanostructured crystalline aggregates by changing the solvent quality. BA molecules dissolved in a good solvent spontaneously aggregate upon the incremental addition of a poor solvent. The observed multilayered structural arrangement of the crystalline assemblies bearing nanostructured lamellar surface topologies pursues the multitude of complex architectures previously reported for steroidal bile compounds. To bridge the gap between the molecular and macroscopic length scales, we have combined spectroscopic (UV−vis, CD, and FTIR), scattering (WAXS), and single-molecule imaging (AFM) techniques. The present results can provide additional clues for the elucidation of the self-assembled structures of chiral facial amphiphiles, as well as to generate new perspectives of potential uses and functionalities.

■ CONCLUSIONS

The self-assembly behavior of naturally occurring mono-, di-, and trihydroxyl bile acids has been investigated based on their spontaneous self-association in solution. Starting from molecular solutions in either EtOH or DMSO as good solvents, the aggregation was induced by a change in the solvent quality

dx.doi.org/10.1021/la300384u | *Langmuir* 2012, 28, 5999−6005

upon the incremental addition of H_2O as a poor solvent. The transformation to cloudy dispersions was faster and more intense for BAs with a lower state of hydroxylation. An increasing number of OH groups and a concomitant higher aqueous solubility in contrast promoted the dissociation of bile acid molecules as indicated by a decreasing pH value of the solvent media, while diminishing the formation of aggregates. The absence of carboxylate stretching vibrations in FTIR spectra from the solid-state aggregates indeed confirms protonated states of aggregated molecules.

Self-assembled bile acids established different macroscopic aggregate morphologies and various microstructures revealing birefringence under crossed polarizers. On a molecular level, the BA assemblies were essentially arranged in multilayers, presenting nanostructured lamellar topologies of differently oriented domains or a rather flat surface, depending on the type of BA, cosolvent, and experimental conditions applied. The complex architecture of the supramolecular bile acid assemblies was also observed by the large number of sharp peaks in the WAXS scattering pattern, indicating the presence of highly crystalline solid-state aggregates. The greatest features in the assemblies of $d = 2\pi/q$ varying from 0.9 to 1.5 nm are in the range of the smallest lattice spacing of the nanostructured surface topologies observed by AFM experiments, and correspond to about the long axis molecular length of the BA molecules. Regular lamellar lattice spacing of about 3 nm is accordingly suggested to comprise two lengthwise associated molecules. In support of this scenario, the carbonyl stretching from the COOH groups observed in the FTIR spectra suggested self-assembled units of dimeric BAs with H-bonded carboxylic groups. The hierarchical configuration of the complex architecture of supramolecular BA assemblies is understood to arise from the lengthwise association in repeating units of H-bonded dimers, forming 2D layers of lamellar nanostructures driven by intermolecular H-bonding between hydroxyl groups on the concave α-faces of facially amphiphilic molecules.

The supramolecular assemblies of BAs unifying characteristics of facial amphiphilicity, chirality, and biocompatibility, offer a great potential in host−guest chemistry, material science and nanotechnology. The design of systems composed of steroidal compounds requires a detailed understanding of the underlying driving forces of the self-assembly and the resulting complex, hierarchical aggregate organization. The present findings may contribute to the understanding of the hierarchical structural arrangement of self-assembled pristine BAs having important implications in the design of tailor-made nanostructures and in the understanding of the physiological and pharmacological role of steroidal aggregates.

■ ASSOCIATED CONTENT

Supporting Information

UV−vis absorption and CD spectra (Figure SI-1), FTIR spectra (Figure SI-2), WAXS spectra (Figure SI-3), 3D chemical structures of bile acids (Figure SI-4), AFM images (Figures SI-5 to SI-11), and tables of scattering vector q values from WAXS patterns with the corresponding AFM and FFT results (Table SI-1 and Table SI-2). This material is available free of charge via the Internet at http://pubs.acs.org.

■ AUTHOR INFORMATION

Corresponding Author

*E-mail: raffaele.mezzenga@hest.ethz.ch.

Notes

The authors declare no competing financial interest.

■ ACKNOWLEDGMENTS

We thank the Swiss National Science Foundation (SNF) for financial support.

■ REFERENCES

(1) Monte, M. J.; Marin, J. J. G.; Antelo, A.; Vazquez-Tato, J. Bile acids: Chemistry, physiology, and pathophysiology. *World J. Gastroenterol.* **2009**, *15*, 804−816.

(2) Mukhopadhyay, S.; Maitra, U. Chemistry and biology of bile acids. *Curr. Sci.* **2004**, *87*, 1666−1683.

(3) Mann, J. *Secondary Metabolism*, 2nd ed.; Oxford University Press: Oxford, U.K., 1987; pp 95−172.

(4) Madenci, D.; Egelhaaf, S. U. Self-assembly in aqueous bile salt solutions. *Curr. Opin. Colloid Interface Sci.* **2010**, *15*, 109−115.

(5) Roda, A.; Fini, A. Effect of Nuclear Hydroxy Substituents on Aqueous Solubility and Acidic Strength of Bile Acids. *Hepatology* **1984**, *4*, 72S−76S.

(6) Small, D. M. Size and Structure of Bile Salt Micelles. In *Molecular Association in Biological and Related Systems*; American Chemical Society: Washington, DC, 1968; Vol. *84*, pp 31−52.

(7) Terech, P.; de Geyer, A.; Struth, B.; Talmon, Y. Self-Assembled Monodisperse Steroid Nanotubes in Water. *Adv. Mater.* **2002**, *14*, 495−498.

(8) Tamhane, K.; Zhang, X.; Zou, J.; Fang, J. Assembly and disassembly of tubular spherulites. *Soft Matter* **2010**, *6*, 1224−1228.

(9) Ramanathan, N.; Currie, A. L.; Colvin, J. R. Formation of Helical Microfibrils from a Steroid Acid Complex. *Nature* **1961**, *190*, 779−781.

(10) Qiao, Y.; Lin, Y.; Wang, Y.; Yang, Z.; Liu, J.; Zhou, J.; Yan, Y.; Huang, J. Metal-Driven Hierarchical Self-Assembled One-Dimensional Nanohelices. *Nano Lett.* **2009**, *9*, 4500−4504.

(11) Wang, X.; Lu, Y.; Duan, Y.; Meng, L.; Li, C. Helical Crystals with a Sixfold Screw Axis. *Adv. Mater.* **2008**, *20*, 462−465.

(12) Sánchez-Ferrer, A.; Adamcik, J.; Mezzenga, R. Edible supramolecular chiral nanostructures by self-assembly of an amphiphilic phytosterol conjugate. *Soft Matter* **2012**, *8*, 149−155.

(13) Wang, R.; Geiger, C.; Chen, L.; Swanson, B.; Whitten, D. G. Direct Observation of Sol-Gel Conversion: The Role oft he Solvent in Organogel Formation. *J. Am. Chem. Soc.* **2000**, *122*, 2399−2400.

(14) Pal, A.; Basit, H.; Sen, S.; Aswal, V. K.; Bhattacharya, S. Structure and properties of two component hydrogels comprising lithocholic acid and organic amines. *J. Mater. Chem.* **2009**, *19*, 4325−4334.

(15) Rich, A.; Blow, D. M. Formation of a Helical Steroid Complex. *Nature* **1958**, *182*, 423−426.

(16) Blow, D. M.; Rich, A. Studies on the Formation of Helical Deoxycholate Complexes. *J. Am. Chem. Soc.* **1960**, *82*, 3566−3571.

(17) Johnson, P. L.; Schaefer, J. P. The Crystal and Molecular Structure of an Addition Compound of Cholic Acid and Ethanol. *Acta Crystallogr.* **1972**, *28*, 3083−3088.

(18) Bertolasi, V.; Ferretti, V.; Fantin, G.; Fogagnolo, M. Solid state molecular assemblies of five bile acid derivatives. *Z. Kristallogr.* **2008**, *223*, 515−523.

(19) Miyata, M.; Tohnai, N.; Hisaki, I. Crystalline Host-Guest Assemblies of Steroidal and Related Molecules: Diversity, Hierarchy, and Supramolecular Chirality. *Acc. Chem. Res.* **2007**, *40*, 694−702.

(20) Brotherhood, P. R.; Davis, A. P. Steroid-based anion receptors and transporters. *Chem. Soc. Rev.* **2010**, *39*, 3633−3647.

(21) Virtanen, E.; Kolehmainen, E. Use of Bile Acids in Pharmacological and Supramolecular Applications. *Eur. J. Org. Chem.* **2004**, 3385−3399.

(22) Zhu, X. X.; Nichifor, M. Polymeric Material Containing Bile Acids. *Acc. Chem. Res.* **2002**, *35*, 539−546.

(23) Pretsch, E.; Bühlmann, P.; Affolter, C. *Structure Determination of Organic Compounds − Tables of Spectral Data*, 3rd ed.; Springer Verlag: Berlin, Germany, 2000; pp 385−404.
(24) *CRC Handbook of Chemistry and Physics*, 92nd ed.; CRC Press: Boca Raton, FL, 2011; pp 94−103.
(25) Kasal, A.; Budesinsky, M.; Griffiths, W. J. Spectroscopic Methods of Steroid Analysis. In *Steroid Analysis*, 2nd ed.; Springer Verlag: Dordrecht, Netherlands, 2010; pp 27−161.